RESEARCH ARTICLE doi.org/10.1002/adsc.202200403 Advanced Synthesis & Catalysis

# Enantioselective Synthesis of Pharmaceutically Relevant Bulky Arylbutylamines Using Engineered Transaminases

Yuriy V. Sheludko,[a] Sjoerd Slagman,[a] Samantha Gittings,[b] Simon J. Charnock,[b] Henrik Land,[c, d] Per Berglund,[c] and Wolf-Dieter Fessner[a,*]

[a] Institut für Organische Chemie und Biochemie, Technische Universität Darmstadt, Darmstadt, 64287, Germany
Tel: +49 6151 16-23640
E-mail: fessner@tu-darmstadt.de
[b] Prozomix Limited, West End Industrial Estate, Haltwhistle, Northumberland, NE49 9HA, UK
[c] KTH Royal Institute of Technology, School of Engineering Sciences in Chemistry, Biotechnology and Health (CBH), Department of Industrial Biotechnology, AlbaNova University Center, SE-106 91, Stockholm, Sweden
[d] Department of Chemistry, Ångström Laboratory, Uppsala University, SE-751 20, Uppsala, Sweden

Manuscript received: April 13, 2022; Revised manuscript received: June 15, 2022;
Version of record online: July 20, 2022

Supporting information for this article is available on the WWW under https://doi.org/10.1002/adsc.202200403



**Abstract:** ATAs engineered for having an enlarged small binding pocket were applied for the synthesis of enantiomerically pure (*R*)-benzo[1,3]dioxol-5-yl-butylamine, a chiral component of human leukocyte elastase inhibitor DMP 777 (L-694,458). Kinetic resolution of the racemic amine was performed by using the L59A variant of the (*S*)-selective ATA from *Chromobacterium violaceum* (*Cv*-ATA), providing the residual (*R*)-enantiomer in excellent yield and >99% *ee*. At moderate enzyme loading and absence of co-solvent, high volumetric productivity of 0.22 mol $L^{-1}$ $h^{-1}$ (42.5 g $L^{-1}$ $h^{-1}$) was achieved. Complementarily, the (*S*)-enantiomer was generated via kinetic resolution using the (*R*)-selective ATA-117-Rd11 from *Arthrobacter sp.* with acetone as the amino acceptor. In an alternative approach, we employed ATA-117-Rd11 for the asymmetric amination of the prochiral ketone precursor, which at 86% conversion gave the (*R*)-benzo[1,3]dioxol-5-yl-butylamine with excellent >99% *ee*. We further evaluated the utility of *Cv*-ATA L59A for the asymmetric synthesis of pharmaceutically relevant (*S*)-1-phenylbutan-1-amine, a chiral component of the deubiquitinase inhibitor degrasyn (WP1130). The enzyme showed good tolerance to high concentrations of isopropylamine, producing (*S*)-1-phenylbutan-1-amine in enantiomerically pure form (>99% *ee*).

**Keywords:** Aminotransferase; Biocatalysis; Chiral amines; Kinetic resolution; Protein engineering

## Introduction

The chiral amine moiety is prevalent in numerous natural and synthetic compounds of pharmaceutical and agrochemical value and often determines their biological activity.[1] Among 200 small-molecule pharmaceutical blockbusters in 2020, more than 30% included a chiral amine group in their structures.[2] Exemplary components are found in the human leukocyte elastase inhibitor DMP 777 (L-694,458), a promising candidate for the treatment of cystic fibrosis, rheumatoid arthritis and chronic obstructive pulmonary disease,[3] as well as of deubiquitinase inhibitor degrasyn (WP1130), possessing anticancer and antibacterial activity against multi-resistant *Staphylococcus aureus*[4] (Figure 1). Besides, chiral amines are widely used as ligands or organo-catalysts for asymmetric chemical synthesis.[5]

While notable achievements have been realized in the chemical synthesis of chiral primary amines,[6] development of biocatalytic methods for the stereoselective amination of a prochiral ketone precursor offers an environment-friendly alternative for industrial processes. Among the enzymes that are capable of

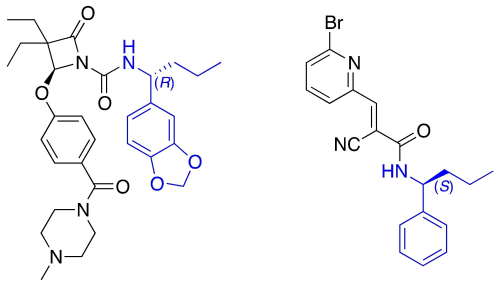


**Figure 1.** Exemplary chiral arylbutylamine motifs in the structure of small molecule pharmaceuticals.

performing such conversion, transaminases (TAs) are attractive catalysts due to their robustness, outstanding enantioselectivity and independence from consumable co-factors. Over recent decades, a plethora of prokaryotic enzymes were discovered that can be applied for efficient biocatalytic transformation of a wide variety of amine substrates of scientific and industrial importance.[7] Amine transaminases (ATAs) are a subgroup of ω-TAs ((*S*)- and (*R*)-selective, class III and IV transaminase family, respectively[8]) that are capable of converting substrates lacking a carboxyl moiety. Therefore, ATAs are of special value for biocatalytic applications due to the broad range of acceptable carbonyl compounds.

Substrate scope and enantioselectivity of TAs are determined by the spatial structure of the active center, which is formed by residues from both subunits at the interface of the homodimeric enzyme. Substrate orientation depends on its relative fit to match a large (L) and a small (S) binding pocket, while the absolute amine configuration is controlled by the direction of amine transfer mediated by a pyridoxal-5′-phosphate (PLP) cofactor.[9] The L-pocket of native ATAs is large enough to embrace bulky aryl or even biaryl substrates[10] and can adapt both hydrophobic as well as polar groups; the capacity of the S-pocket is usually very limited and can accommodate an ethyl moiety at maximum.[11] As a rare exception from this rule, the TA from *Paracoccus denitrificans* can accept up to a butyl group in its S-pocket, but only if an α-carboxylate binds to an arginine moiety in the corresponding L-pocket.[12]

The first landmark engineering of an (*R*)-selective ATA was reported toward the manufacture of anti-diabetic drug sitagliptin, where the enzyme from *Arthrobacter* sp. was extensively engineered via several rounds of directed evolution to achieve drastic improvements in enzyme activity with the bulky substrate pro-sitagliptin ketone, as well as robustness under harsh industrial conditions.[13] Numerous later studies achieved substantial expansion of the substrate scope for both (*R*)- and (*S*)-selective ATAs towards bulky compounds especially by modifying the S-pocket geometry.[14] However, challenges remain for the use of ATAs in the scalable synthesis of chiral α-aryl amines from the corresponding phenones caused by the poor water solubility of the substrates possible substrate inhibition of the enzyme, and the thermodynamically unfavorable situation from ketone stabilizing aryl conjugation.[15] For example, the value of the equilibrium constant for the transamination of acetophenone (**1**) was estimated at $10^{-3}$ – $10^{-5}$ for the substrate/product pairs of L-alanine (**3**)/acetophenone (**1**) and pyruvate (**4**)/(*S*)-1-phenylethanamine (1-methylbenzylamine or MBA), **2**).[15b,16] In addition, relative conversion rates of ATAs with ketones are several orders of magnitude lower than the corresponding activities for aldehydes or α-keto acids.[17] Recently, we engineered the highly effective (*S*)-specific ATA from *Chromobacterium violaceum*[18] (*Cv*-ATA) to accommodate more bulky substrates. In the *Cv*-ATA L59A /F88A variant, the S-pocket was sufficiently enlarged to accept the doubly bulky substrate 1,2-diphenylethanamine.[15c] In the course of this study using a series of fluorogenic substrates for highly sensitive detection,[19] we observed that the single replacement L59A initiated significantly higher activity against 1-(6-methoxy-2-naphthyl)butanamine (**7**) as compared to the L59A /F88A variant, whereas the wild-type enzyme showed barely any activity.[15c] This inspired us to investigate the suitability of *Cv*-ATA L59A for the preparation of enantiomerically pure arylbutylamines **5** and **6** (Figure 2) as exemplary, valuable building blocks for pharmaceutical synthesis.

In view of the thermodynamic obstacles, complementary strategies of both kinetic resolution and direct asymmetric synthesis processes were considered using the (*S*)-selective *Cv*-ATA L59A or (*R*)-selective ATAs, respectively (Scheme 1). For the latter, we screened a commercial panel of genomic and metagenomic TAs.[13a] As a result, both pure enantiomers of **5** could be prepared with *ee* > 99% in fair to excellent yield. In addition, the *Cv*-ATA L59A was evaluated for direct access to the pharmaceutically relevant chiral amine building block (*S*)-**6** from butyrophenone (**9**).

## Results and Discussion

Especially, we focused on the development of an effective protocol for a sustainable enzymatic synthesis of (*R*)-**5** from the corresponding ketone **8** to replace the palladium catalyzed chemical transformation.[3b] Also, access options to its enantiomer (*S*)-**5** were investigated as well as to the structurally related building block (*S*)-**6**.

*Cv*-ATA was used for experiments exploiting (*S*)-selectivity; however, (*R*)-selectivity is rather rare in nature. Thus, in an attempt to broaden the biocatalytic toolbox by adding new TAs having both desired (*R*)-

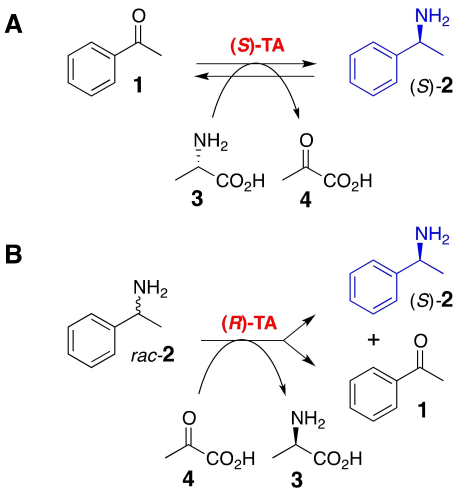


**Scheme 1.** Complementary routes to chiral 1-arylethanamines (blue) *via* direct asymmetric synthesis (A) or kinetic resolution (B).

specificity as well as ATA-type activity we first screened a large commercial library of genomic and metagenomic TAs (192 candidates; Prozomix Ltd, UK) that was designed to cover maximum sequence diversity.

## Screening of a Native TA Library for the Stereoselective Synthesis of (R)-5

In the last decade, a versatile toolbox has been developed for the high-throughput screening of TA activities.[20] A commercial arrayed library of 192 TAs obtained by genome and metagenome mining (PRO-TRANS 001-192) was screened for enzymes that could be utilized for the asymmetric synthesis of (*R*)-**5** (Scheme 1A). Firstly, we screened the panel against (*S*)-**2** and (*R*)-**2** as amino donors using pyruvate (**4**) as amino acceptor for differentiation of (*R*)- and (*S*)-selective TAs. The assay relies on the detection of UV-absorbance from acetophenone (**1**) formation for quantitative estimation of conversion rate.[21] Eleven (*S*)-selective ATAs were found that displayed an activity of 30–112% relative to that of wild-type *Cv*-ATA whereas no promising (*R*)-selective candidate could be identified (Figure S1). The most potent (*R*)-selective enzyme in the panel, PRO-TRANS(113), exhibited some activity against (*R*)-**2** (7% of the *Cv*-ATA activity) but more readily accepted α-amino and keto acid substrates (data not shown), indicating that this enzyme belongs to the α-TA subgroup. These results are in accordance with the distribution of TAs in nature, where the predominant part of the enzymes shows (*S*)-enantioselectivity.[7a]

Secondly, we assayed the TA library against bulky ketone substrate **8** using *p*-nitrobenzylamine (**10**) as a smart amino donor in a colorimetric assay (Figure 2).[22] No or negligible color formation was observed in the **8** containing samples as compared to a control lacking the ketone (Figure S2). These results suggest inapplicability of native ATAs in the panel for the direct stereoselective synthesis of **5**; apparently, there is no appropriate metabolic function in nature that required specificity for similarly bulky substrates (or such enzymes are yet unknown). Therefore, the evaluation of potential synthetic routes to the target compounds was conducted by utilizing the engineered variant of (*R*)-ATA from *Arthrobacter* sp. (ATA-117-Rd11) instead, which offered a suitably enlarged substrate scope and an especially robust nature.[13a]

## Direct Asymmetric Synthesis of (R)-5 Using Engineered ATA-117-Rd11

Efficient amination of α-aryl alkyl ketones remains a challenging task for biocatalysis. Asymmetric synthesis of **6** from butyrophenone (**9**) by engineered ATAs was previously carried out at either low concentration (≤10 mM) or moderate conversion rate (≤50%).[13b,14a–d] Remarkably, the engineered variant ATA-117-Rd11 had showed excellent to moderate yields for the conversion of various bulky ketones (including **9**) that were unreactive with the (*R*)-selective wild-type enzyme from *Arthrobacter* sp.[13b] Thus, we selected this biocatalyst for the synthesis of (*R*)-**5** from the prochiral ketone **8** (Scheme 2) also in view of the enzyme's enhanced activity towards isopropylamine (**11**) as an inexpensive amino donor as

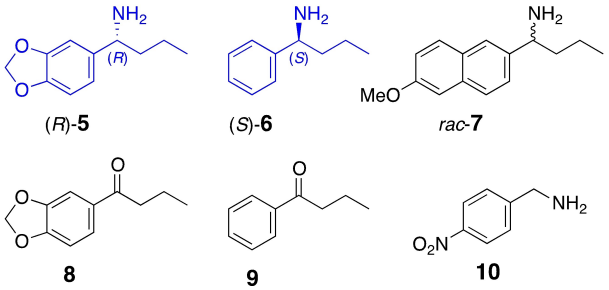


**Figure 2.** Synthetic targets (blue) and substrates utilized for the synthesis (ketones) and activity screening (amines).

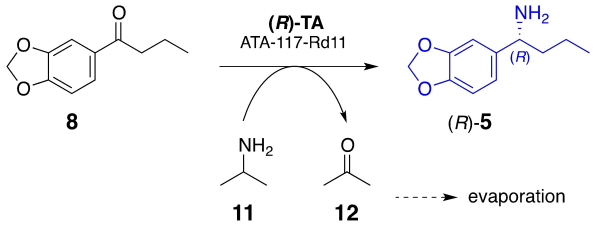


**Scheme 2.** Asymmetric synthesis of (*R*)-**5** using (*R*)-selective ATA-117-Rd11.

well as an outstanding tolerance to elevated temperatures (up to 60 °C), organic co-solvents and alkaline reaction conditions (pH 8–11).[13a]

When incubated with amino donors **2**, **10** or **11** for 17 h, ATA-117-Rd11 achieved 14%, 5% and 15% conversion of **8**, respectively. Consequently, **11** was selected as cost- and process-effective amino donor for subsequent experiments. A high concentration of non-protonated amine was secured by maintaining the reaction mixture at pH 11.0 for maximum efficiency.[23] In a pilot experiment with 250 mM **11**, 10 mM **8**, 40% DMSO and 10 mg/mL ATA-117-Rd11 (cell free extract; CFE), a 70% conversion was achieved after 216 h incubation at 45 °C (Figure 3A), confirming the unusual operational stability of the enzyme under harsh conditions.

Application of an excess amino donor in combination with product/co-product removal is an efficient way to shift a thermodynamically unfavorable amination equilibrium to maximize conversion of a stabilized ketone.[24] Acetone (**12**), generated from **11** as amino donor, can be efficiently eliminated from the reaction mixture either enzymatically or by using various physical procedures.[25] In view of the low volatility of **8** and the stability of the enzyme, we chose incubation at slightly elevated reaction temperatures and reduced pressure for continuous removal of **12** as recommended.[13b,14b]

Preparative-scale synthesis was performed in a total reaction volume of 20 mL containing 50 mM **8** at 45 °C and 400 mbar vacuum under magnetic stirring. The DMSO level had to be raised to 50% to aid in the solubilization of the ketone. The reaction was stopped after 216 h of incubation when conversion had reached 86% (Figure 3B). Product was isolated by liquid-liquid acid-base extraction (90% extraction yield) followed by preparative RP-chromatography to eliminate residual DMSO (70% extraction yield). Solvent evaporation gave 141 mg of pure (*R*)-**5** as its formate salt (61% overall yield; *ee* > 99%; Figure S3–S5).

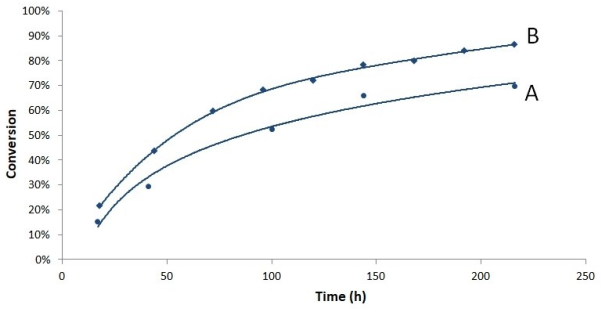


**Figure 3.** ATA-117-Rd11 catalyzed conversion of **8** under different process conditions. The conversion was estimated by quantifying the concentration of **8** *via* HPLC analysis. Reaction conditions: A) total volume 0.6 mL; 250 mM **11**, 10 mM **8**, 0.5 mM PLP, 40% DMSO and 10 mg mL$^{-1}$ ATA-117-Rd11 CFE in 0.1 M $KP_i$ buffer; pH 11.0; 45 °C, 450 rpm; B) total volume 20 mL; 500 mM **11**, 50 mM **8**, 0.5 mM PLP, 50% DMSO and 25 mg mL$^{-1}$ ATA-117-Rd11 CFE in 0.1 M $KP_i$ buffer; pH 11.0; 45 °C; 400 mbar vacuum; all samples were measured in duplicates.

## Kinetic Resolution of rac-5 by Cv-ATA L59A

Despite the high conversion rate and excellent stereoselectivity, productivity of the asymmetric synthesis of (*R*)-**5** was rather low due to the moderate activity of ATA-117-Rd11 towards ketone **8**. Therefore, the kinetic resolution of readily accessible *rac*-**5**[26] seemed to be a promising alternative. This should profit from good aqueous solubility of the (protonated) amine substrate, avoiding the need for DMSO co-solvent undesired for industrial applications,[15c] and from the energetically more favorable direction to produce a resonance stabilized ketone product (Scheme 3). For optimization of the kinetic resolution, pH and co-solvent tolerance of the variant *Cv*-ATA L59A were examined by using the UV-assay calibrated at the 310 nm absorbance maximum of ketone **8** (Figure S6).

The pH-optimum of *Cv*-ATA L59A was found to be pH 8.0 (Figure 4A), which is intermediate between that of WT (pH 8.5)[27] and the L59A /F88A variant (pH 7.5).[15c] As a compromise to improve aqueous solubility of the amine **5**, the kinetic resolution was nevertheless performed at pH 7.5, where the enzyme retains 90% of its activity (Figure 4A). Similarly, *Cv*-ATA L59A displayed intermediate tolerance to DMSO with its maximum activity at 10% (v/v) DMSO (Figure 4B) as compared to WT (max. activity at 0% DMSO) and the solvent-tolerant L59A /F88A variant (max. activity at 20–30% (v/v) DMSO).[15c] The activity of *Cv*-ATA L59A at 0% DMSO was around 40% of the maximum, which is still acceptable for performing the kinetic resolution in the absence of co-solvent to facilitate downstream processing.

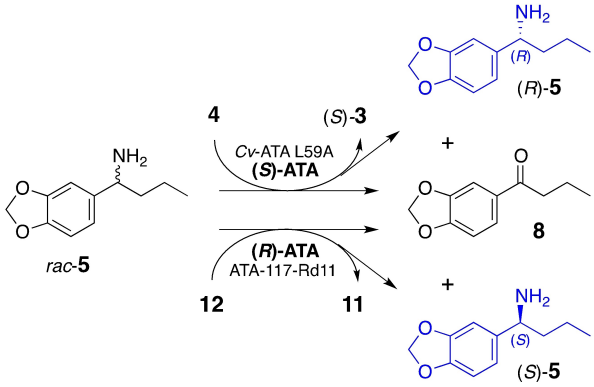


**Scheme 3.** Kinetic resolution of *rac*-**5** using either (*S*)- or (*R*)-selective ATA resulting in (*R*)-**5** or (*S*)-**5**, respectively.

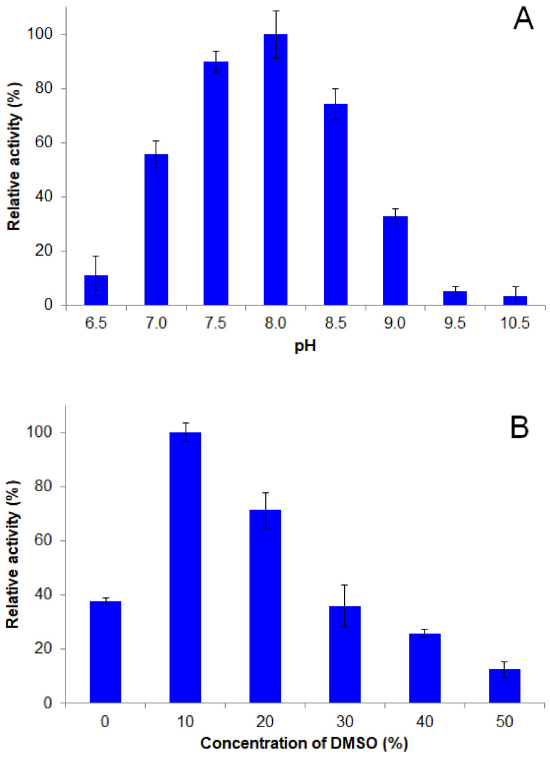


**Figure 4.** Biochemical characterization of *Cv*-ATA L59A with respect to the influence of pH (A) and DMSO concentration (B) on the generation of **8**. Activity at pH 8.0 (A; 0.24 ± 0.02 μmol min$^{-1}$ mg$^{-1}$ of total soluble protein (TSP)) and at 10% DMSO (B; 1.11 ± 0.04 μmol min$^{-1}$ mg$^{-1}$ of TSP) was set as 100%, respectively. Bars represent standard deviation of a minimum of three replicates. Full details of experimental conditions are given in the Experimental Section.

Interestingly, *Cv*-ATA L59A showed slightly higher thermal stability ($T_m$ = 82.9 °C) than the wild type enzyme ($T_m$ = 80.6 °C) as determined by nanoDSF analysis[28] and good stability in the presence of 10% - 20% (v/v) acetone (Figure S7).

In an analytical-scale experiment with 0.2 M *rac*-**5**, 0.2 M pyruvate (**4**), and 2.75 mg mL$^{-1}$ purified *Cv*-ATA L59A at 30 °C (100 mM $KP_i$ buffer, pH 7.5, no co-solvent), we found that complete resolution had occurred already within 15 min of incubation and residual (*R*)-**5** had an *ee* > 99%. Higher concentration of substrates at constant enzyme load resulted in incomplete resolution (Figure S8–S9). Rapid accumulation of ketone **8**, which has poor aqueous solubility, may accelerate the conversion rate by pulling the equilibrium towards the product side. On the other hand, the fast generation of a non-homogeneous mixture by formation of **8** is accompanied by protein precipitation. Dropwise substrate addition to a biphasic reaction system did not improve the process yield (data not shown). For preparative scale-up, kinetic resolution of *rac*-**5** was performed in an 8 mL reaction volume containing 0.2 M **4** and 2.75 mg mL$^{-1}$ purified *Cv*-ATA L59A. The amine (*rac*-**5**, 309 mg) was added dropwise over 15 min up to a final 0.2 M concentration. Immediately after complete substrate addition, $ee_R$ was estimated at 93% and reached > 99% within a further 10 min when the reaction was stopped. Unreacted amine was isolated by extraction to give 140 mg (91% yield, based on the residual enantiomer) of enantiomerically pure (*R*)-**5** ($ee_R$ > 99%) (Figure S10–S12).

## Kinetic Resolution of rac-5 by ATA-117-Rd11

For the production of the complementary enantiomer (*S*)-**5**, we decided to perform the kinetic resolution of *rac*-**5** by using ATA-117-Rd11 with **12** as the amino acceptor (Scheme 3). Acetone (**12**) as a co-substrate has advantages against pyruvate (**4**) such as lower cost and easier handling upon downstream processing, although the native activity of ATAs towards **4** usually surpasses that for **12** by manifold.[15b] In a comparison of the enzymes we found that activity of *Cv*-ATA L59A towards **12** was only about 1% of that for **4**, while the activity of ATA-117-Rd11 was of similar magnitude towards **12** and **4** (Figure 5). Low activity of ATA-117-Rd11 with **4** is due to a G136F mutation introduced to enlarge the L-pocket; however, this alters the conformation of the loop 129–145 responsible for recognition of **4** in (*R*)-selective ATAs.[13c] On the other hand, high tolerance of the enzyme to large concentrations of co-solvents and **11** was expected to facilitate an efficient transamination of **12**. Utilization of **12** as an amino acceptor for preparative TA-catalyzed biotransformations is uncommon, likely due to the low driving force of the conversion and moderate enzyme activities. To the best of our knowledge, only a single example of the kinetic resolution of *rac*-**2** with acetone

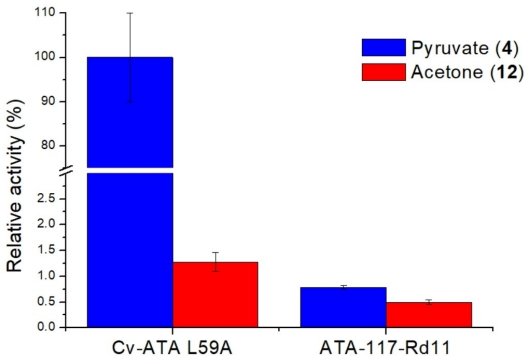


**Figure 5.** Activities of *Cv*-ATA L59A and ATA-117-Rd11 towards *rac*-**5** (1 mM) as an amino donor and pyruvate (**4**; 1 mM) or acetone (**12**; 20 mM) as amino acceptor. The activity of *Cv*-ATA L59A towards pyruvate was set as 100% (0.54 ± 0.05 μmol min$^{-1}$ mg$^{-1}$). Bars represent the standard deviation of a minimum of three replicates. Full details of experimental conditions are given in the Experimental Section.

(**12**) catalyzed by (*R*)-ATA from *Mycobacterium vanbaalenii* has been reported.[29]

In the pilot experiment, ATA-117-Rd11 displayed good tolerance to 1 M acetone (**12**), and after 4 h incubation resolution to (*S*)-**5** reached *ee* 76%. Employing significantly higher concentration of **12** resulted in enzyme inhibition and poor resolution (Figure S13).

Therefore, in a preparative run the kinetic resolution was performed in a 10 mL reaction volume containing 1.2 M **12** and 0.1 M *rac*-**5** (192 mg) with 30 mg mL$^{-1}$ ATA-117-Rd11 CFE. After 6 h incubation time, (*S*)-**5** reached >99% *ee* when the reaction was stopped (Figure S14). Extractive work-up furnished 53 mg (59% yield, based on the residual enantiomer) of enantiomerically pure (*S*)-**5** ($ee_S$ >99%) (Figure S15–S17).

## Asymmetric Synthesis of Both Enantiomers of 6 using Cv-ATA L59A or ATA-117-Rd11

Examples of enzymatic amination of butyrophenone (**9**) by engineered ATAs have been reported at moderate conversion rate and/or reaction scale.[13b,14b,c,17] Recently, asymmetric amination of 50 mM isobutyrophenone was performed using a triple mutant of (*S*)-ATA from *Ochrobactrum anthropic*. The yield reached 45.6%, probably limited by approaching the equilibrium.[30]

To evaluate *Cv*-ATA L59A for the stereoselective synthesis of the amine (*S*)-**6**, we tested the enzyme for conversion of **9** in the presence of two potential amino donors (*S*)-MBA (**2**) and isopropylamine (**11**) (Scheme 4). Although the enzyme activity of *Cv*-ATA L59A for **2** was higher as compared to **11** (Figure 6A; 0.033 ± 0.001 μmol min$^{-1}$ mg$^{-1}$ and 0.007 ± 0.001 μmol min$^{-1}$ mg$^{-1}$, respectively), the latter amino donor ensured a better conversion rate (83% as determined by HPLC; Figure 6B) when applied at 100-fold excess (0.5 M) over **9**. The specific activity of *Cv*-ATA L59A towards **9** and **11** surpassed the corresponding value of ATA-117-Rd11 by an order of magnitude (Figure 6A) but was slightly inferior to that of the (*S*)-ATA variant from *O. anthropic* harboring a triple

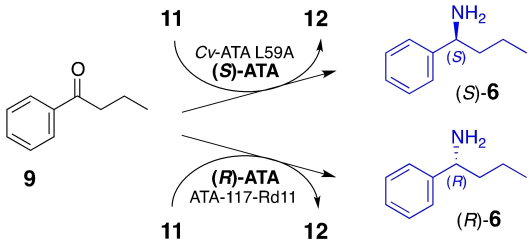


**Scheme 4.** Asymmetric synthesis of (*S*)- and (*R*)-**6** using *Cv*-ATA L59A and ATA-117-Rd11, respectively.

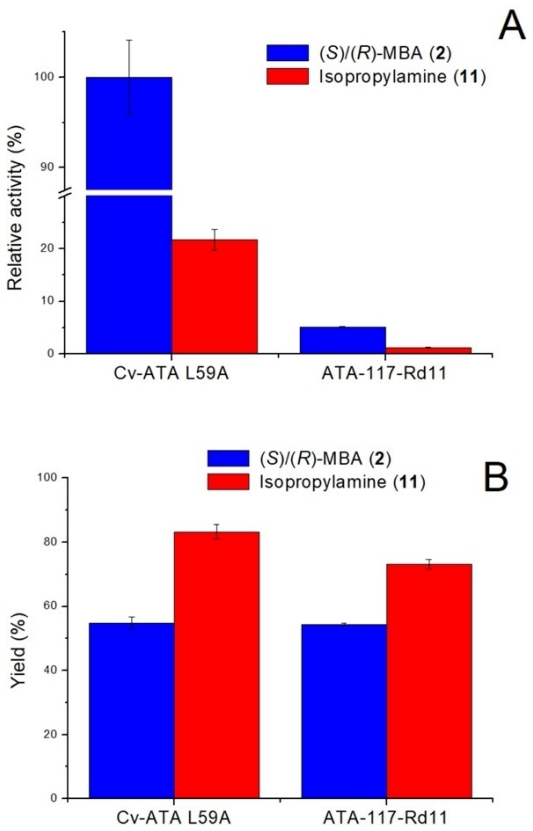


**Figure 6.** Activities of *Cv*-ATA L59A and ATA-117-Rd11 towards (*S*)- or (*R*)-**2** (5 mM) and **11** (0.5 M), respectively, as an amino donor, and **9** (5 mM) as amino acceptor: **A**) relative activity; **B**) yield. The activity of *Cv*-ATA L59A towards (*S*)-**2** was set as 100% (0.033 ± 0.001 μmol min$^{-1}$ mg$^{-1}$). Bars represent the standard deviation of a minimum of two replicates. Full details of experimental conditions are given in the Experimental Section.

mutation (0.028 μmol min$^{-1}$ mg$^{-1}$; recalculated from ref.[30]).

For scaling up the process, we tested the conversion of 50 mM **9** in the presence of 1 M, 1.5 M and 2 M **11** (20-, 30- and 40-fold excess, respectively). We noticed that the concentration of **11** above 1.5 M inhibited the enzyme and decreased the yield (Figure S18). The preparative conversion was therefore carried out in a 9 mL volume containing 50 mM **9**, 1.5 M **11** and 4.8 mg mL$^{-1}$ purified *Cv*-ATA L59A . The reaction was stopped after 24 h when approaching the equilibrium (42% conversion), yielding enantiomerically pure (*S*)-**6** (4 mg, 7% overall yield, $ee_S$ >99%) (Figure S19–22). The moderate conversion rate can be explained by insufficient excess of the amino donor to further drive the equilibrium. Selective removal of the co-product **12** under reduced pressure is not an option for volatile ketone substrates, as reported for acetophenone (**1**).[24a] Henry's constant of **9** even surpasses that of **1** (1.73E-05 atm m$^3$ mole$^{-1}$ and 1.04E-05 atm m$^3$

mole$^{-1}$, respectively), indicating its higher volatility. Thus, alternative strategies for withdrawal of **12** (e.g., enzymatic removal[31]) would be required to further improve the conversion rate.

In a complementary approach, the kinetic resolution of *rac*-**6** was also performed by using ATA-117-Rd11 with acetone as the amino acceptor as described above. After 72 h incubation, (*S*)-**6** reached 96% *ee* when the reaction was stopped (Figure S24). Extractive workup furnished 25 mg of (*S*)-**6** (86% yield, based on the residual enantiomer; $ee_S = 96\%$) (Figure S25–S27). We suppose that the lower stereoselectivity of ATA-117-Rd11 towards *rac*-**6** originates in the less bulky phenyl moiety (as compared to *rac*-**5**), which renders the two hydrophobic moieties at the amine functionality more difficult to differentiate for this enzyme.

## Conclusions

We have studied two ATAs of complementary stereoselectivity, engineered for having an enlarged small binding pocket, for the synthesis of two arylbutylamines **5** and **6** as pharmaceutically relevant building blocks in enantiomerically pure form, considering both direct asymmetric synthesis and kinetic resolution strategies.

For the direct asymmetric synthesis of (*R*)-**5**, which is a key chiral component of human leukocyte elastase inhibitor DMP 777 (L-694,458), we employed the commercial (*R*)-selective *Arthrobacter* ATA-117-Rd11. Under optimized conditions with removal of acetone generated as a co-product, 86% conversion of prochiral ketone **8** gave (*R*)-**5** with excellent purity (>99% *ee*). However, the productivity of the process (0.17 mmol L$^{-1}$ h$^{-1}$ (0.033 g L$^{-1}$ h$^{-1}$) was rather inefficient due to the thermodynamically unfavorable equilibrium character of the reaction. No alternative (*R*)-selective ATA could be identified by screening of the commercial PRO-TRANS library, despite a broad coverage of TA sequence space.

In a complementary approach, we applied the recently created *Cv*-ATA L59A variant, enabled to accept a bulky butyl group in the S-pocket, towards the kinetic resolution of racemic **5**.[15c] The variant displayed a shift in pH optimum, improved co-solvent tolerance and a slightly higher thermal stability as compared to the wild type enzyme. The kinetic resolution of 0.2 M (39 g L$^{-1}$) *rac*-**5** was carried out at a moderate enzyme loading (2.75 g L$^{-1}$) with amino-transfer to pyruvate in the absence of co-solvent, leaving the unreacted (*R*)-enantiomer in excellent yield and >99% *ee* after a very short incubation time of only 25 min. The outstandingly high volumetric productivity of this reaction (0.22 mol L$^{-1}$ h$^{-1}$ or 42.5 g L$^{-1}$ h$^{-1}$), still offers room for further improvement of the process efficiency, such as by enzyme immobilization and/or compartmentalization of the reaction products. Similarly, the corresponding enantiomer (*S*)-**5** was obtained *via* kinetic resolution of *rac*-**5** but using ATA-117-Rd11 instead and acetone (**12**) as an industrially attractive amino acceptor.

We also evaluated the utility of *Cv*-ATA L59A for the asymmetric synthesis of the pharmaceutically relevant amine (*S*)-**6**. Enzyme activity was slightly lower than the reported value of the triple ATA mutant from *O. anthropic*.[30] *Cv*-ATA L59A displayed tolerance to isopropylamine (**11**) concentrations of up to 1.5 M and produced enantiomerically pure (*S*)-**6** (> 99% *ee*) from butyrophenone (**9**) in satisfactory overall yield, which was limited by equilibrium effects.

The reported data suggest that minimum rational engineering of an ATA seems to be sufficient for obtaining an efficient biocatalyst with expanded substrate scope and improved robustness.[15c] Thus, the coordinated optimization of enzyme characteristics and suitable process configuration can allow for the biocatalytic synthesis of sterically and thermodynamically demanding amine building blocks with high volumetric productivity, excellent stereoselectivity and moderate enzyme loading.

## Experimental Section

### Synthesis of Benzo[1,3]dioxol-5-yl-butylamine rac-(5)

Racemic amine **5** ($ee_R = 5 \pm 1\%$) was prepared according to Amato et al.[26] with few modifications (see Supporting Information S1.2 for details).

$^1$H NMR (300 MHz, $CDCl_3$) $\delta$ 6.86 – 6.79 (m, 1H), 6.74 – 6.72 (m, 2H), 5.92 (s, 2H), 3.80 (t, $J$=6.9 Hz, 1H), 1.58 (td, $J$= 12.8, 6.3, 2.9 Hz, 2H), 1.47 (brs, 2H), 1.38 – 1.12 (m, 2H), 0.89 (t, $J$=7.3 Hz, 3H). $^{13}$C NMR (75 MHz, $CDCl_3$) $\delta$ 147.67, 146.26, 140.93, 119.47, 107.96, 106.61, 100.83, 55.83, 41.89, 19.74, 14.01.

### Enzyme Expression and Purification

*Escherichia coli* BL21 (DE3) competent cells were transformed with a pET28(α+) vector containing the sequence encoding *Cv*-ATA (NCBI: WP 011135573.1) L59A protein linked to a polyhistidine tag. After overnight incubation on solid LB medium (50 μg/mL kanamycin), a positive colonies were picked, cultured in liquid LB (50 μg/mL kanamycin) at 37 °C for 6 h and stored in 16% glycerol at −80 °C. SDS-PAGE analysis confirmed a high expression level of the recombinant protein (>50% total soluble protein (TSP), Figure S28). A larger-scale expression was performed in baffled 2 L flasks with 0.5 L autoinduction medium ZYM-5052[32] (50 μg/mL kanamycin, lacking trace metals) in an Ecotron shaker (Infors AG, Bottmingen, CH) for 6 h at 37 °C, followed by 18 h at 30 °C and 220 rpm. Cells were harvested using a Thermo Scientific™ Contifuge™ Stratos™ centrifuge (Fisher Scientific GmbH., Schwerte, Germany) and frozen at –20°C overnight. Cells were thawed in 20 mM sodium phosphate buffer (pH 7.4) supple-

mented with 0.5 mg mL$^{-1}$ lysozyme and 5 U mL$^{-1}$ DNase I at 37 °C for 30 min. The lysate was adjusted to 0.5 mM PLP and 1 mM dithiothreitol and incubated for 1 h at room temperature under magnetic stirring. After incubation, the lysate was adjusted to 0.5 M NaCl and centrifuged at 4 °C and 12.000 g for 30 min for clarification. The supernatant was adjusted to 30 mM imidazole and loaded onto a pre-equilibrated HisTrap™ FF column containing Ni Sepharose® 6 Fast Flow (Cytiva Europe GmbH, former GE Healthcare, Freiburg, Germany). The column was washed, and the target protein was eluted with a buffer containing 20 mM sodium phosphate, 0.5 M NaCl and 50 mM EDTA (pH 7.4). The buffer was exchanged with 50 mM HEPES (pH 7.5) containing 0.5 mM PLP by size exclusion chromatography, and the sample was freeze-dried.

The sequence encoding ATA-117-Rd11 (PDB: 5FR9 A) linked to a poly-His tag was ligated into a pET28(α+) vector, and the construct was transformed into *Escherichia coli* BL21 (DE3) competent cells for protein overexpression. The prepared cell free extract contained 50 ± 2% TSP as determined by bicinchoninic acid assay and thereof around 60% target protein (estimated by SDS-PAGE).

A commercial panel PRO-TRANSP (Prozomix Limited, Haltwhistle, UK) of 192 TAs was provided in MTP format as lyophilised cell-free extracts (1 mg/well). Concentration of TCP in the samples was 70 ± 13% (determined by bicinchoninic acid assay) and thereof 40–80% target protein (estimated from SDS-PAGE of the selected samples).

## HPLC Analysis

RP-HPLC analyses were carried out with a Shimadzu LC20AT HPLC system (Shimadzu U.S.A. Manufacturing Inc., Canby, USA) using an XBridge™ C18 (Waters, Milford, USA) analytical column (3 × 150 mm, 3.5 µm) and the mobile phase consisting of 0.1% (v/v) formic acid (A) and 0.1% (v/v) formic acid in acetonitrile (B). For the separation, the following binary gradient elution program was applied (% B): 10 within 3 min; 10–90 within 12 min. The column was flushed with 99% B for 4 min and re-equilibrated with 10% B for 5 min. The flow rate was set to 0.5 mL min$^{-1}$ and absorbance of **8** was detected at 280 nm, absorbance of **1** and **9** at 250 nm. The absorbance of amine **6** was detected at 190 nm.

For chiral HPLC analysis, amines **5** and **6** were derivatized with 9-fluorenylmethyl chloroformate (Fmoc-Cl) as described[33] with minor modifications (see Supporting Information S1.3 for details). Chiral HPLC was performed on a Shimadzu 20A system, using a Lux® Cellulose 1 (Phenomenex, Torrance, USA) column (250 × 4.6 mm, 5 µm) and the mobile phase consisting of a) 5% (v/v) isopropyl alcohol and 0.1% (v/v) diethylamine in acetonitrile (Figure S5, S9 and S10); b) 99% (v/v) acetonitrile and 0.1% (v/v) formic acid (Figure S15) for separation of Fmoc-**5** enantiomers or c) 25% (v/v) isopropyl alcohol and 0.1% (v/v) diethylamine in hexane for separation of Fmoc-**6** enantiomers. The flow rate was set to 0.75 mL min$^{-1}$, the column temperature to 25 °C and absorbance of the products after Fmoc derivatization was detected at 256 nm.

Alternatively, for separation of Fmoc-**6** enantiomers (Figure S27), a mobile phase consisting of 0.1% (v/v) formic acid (A) and 0.1% (v/v) formic acid in acetonitrile (B) was employed, and the following binary gradient elution program was applied (% B): 60–95 within 10 min, 95–99 within 5 min. The column was flushed with 99% B for 5 min and re-equilibrated with 60% B for 4 min. The flow rate was set to 0.75 mL min$^{-1}$, the column temperature to 30 °C and absorbance of the products was detected at 250 nm.

## High-Throughput Screening of a Commercial TA Library

A commercial panel of 192 TAs (PRO-TRANS; Prozomix Ltd, Northumberland, UK) was screened against (*S*)-**2** or (*R*)-**2** as an amino donor and pyruvate (**4**) as an amino acceptor in microtiter plate format, and enzyme activities were detected using UV assay for acetophenone formation.[21] TAs from the panel were also screened against **10** as an amino donor with **8** as an amino acceptor in a qualitative colorimetric assay.[22] Detailed assay protocols are provided as Supporting Information (S1.4).

## Biochemical Enzyme Characterization

To determine pH optimum, co-solvent tolerance and the substrate specificity of the enzymes, we employed a UV assay,[21] adapted for the detection of ketone product **8** in the reaction mixture. Reactions were performed in 96-well UV transparent flat-bottom microtiter plates (Thermo Fisher Scientific, Weaverville, USA) in a total volume of 0.2 mL. The plates were incubated at 30 °C (*Cv*-ATA L59A ) or 45 °C (ATA-117-Rd11), and the absorbance of **8** was detected in a kinetic mode at 310 nm. Specific activity was quantified using a calibration curve built for the standard solutions of **8** (Figure S6).

Analysis of enzyme activity as a function of the pH was performed using universal Davies buffer solutions[34] at a range of pH values between 6.5 and 10.5. Reaction conditions: 1 mM *rac*-**5**, 1 mM **4**, 0.05 mM PLP, 0.03 mg mL$^{-1}$ of purified *Cv*-ATA L59A in 100 mM Davies buffers of different pH values. Specific activity was quantified by the amount of **8** produced in 10 min.

The enzyme tolerance to co-solvents was estimated at a 0–50% (v/v) range of DMSO or acetone concentration. Reaction conditions: 1 mM *rac*-**5**, 1 mM **4**, 0.05 mM PLP, 0–50% (v/v) co-solvent, 0.03 mg mL$^{-1}$ of purified *Cv*-ATA L59A in 100 mM $KP_i$ buffer (pH 7.5). Specific activity was quantified by the amount of **8** produced in 10 min (DMSO) or 20 min (acetone).

Activities of *Cv*-ATA L59A and ATA-117-Rd11 towards *rac*-**5** as an amino donor and pyruvate (**4**) and acetone (**12**) as amino acceptors were determined under the following conditions: 1 mM *rac*-**5**, 1 mM **4** or 20 mM **3**, 0.05 mM PLP, 0.03 mg mL$^{-1}$ of purified *Cv*-ATA L59A or 0.25 mg mL$^{-1}$ of ATA-117-Rd11 CFE in 100 mM $KP_i$ buffer (pH 7.5). The activity was determined by the amount of **8** produced in 5 min (*Cv*-ATA L59A for **4**) or 90 min.

Activities of *Cv*-ATA L59A and ATA-117-Rd11 towards **11** and (*S*)- or (*R*)-**2**, respectively, as amino donors and **9** as an amino acceptor were determined using HPLC. Reaction conditions (total volume 0.4 mL): 0.5 M **11** or 5 mM (*S*)- or (*R*)-**2**, 5 mM **9**, 0.1 mM PLP, 0.9 mg mL$^{-1}$ of purified *Cv*-ATA L59A or

4 mg mL$^{-1}$ of ATA-117-Rd11 CFE in 100 mM $KP_i$ buffer pH 8.0 or pH 11.0 (ATA-117-Rd11 and **11** as an amino donor). The vials were incubated at 30 °C (*Cv*-ATA L59A ) or 45 °C (ATA-117-Rd11) and 450 rpm. Activity was determined by the amount of **6** or **1** produced in 15 min (*Cv*-ATA L59A ) or 30 min (ATA-117-Rd11); the yield was HPLC determined by the residual amount of **9** after 88 h of incubation. Specific activities were quantified using a calibration curve built for standard solutions of **6**, **1** and **9**.

Protein melting point ($T_m$) was calculated from the first derivative of the fluorescence emission intensities at 330 and 350 nm using a Prometheus nanoDSF instrument (NanoTemper Technologies, München, Germany).

### Preparative Synthesis of (R)-5, (S)-5 and (S)-6

Preparative synthesis of (*R*)-**5** was performed in a round-bottom flask with 20 mL reaction volume containing 0.5 M **11**, 50 mM **8**, 0.5 mM PLP, 50% DMSO and 25 mg mL$^{-1}$ ATA-117-Rd11 CFE in 0.1 M $KP_i$ buffer at pH 11.0, 45 °C and 400 mbar vacuum under magnetic stirring. During incubation, the pH value was maintained at 11.0 with 4 M **11**. See also figure captions for specific conditions regarding analytical scale reactions.

For the extraction, pH value of the reaction mixture was adjusted to 1.3 with conc. HCl and precipitated proteins were separated by centrifugation. The supernatant was decanted and extracted two times with equal volumes of ethyl acetate. The aqueous phase was saturated with NaCl, and pH was adjusted to 12.5 with 6 M NaOH. The aqueous phase was extracted two times with equal volumes of ethyl acetate; the organic fractions were combined, dried over magnesium sulfate, and the solvent was rotary evaporated.

The obtained extract was submitted to a preparative RP chromatography. The separation was performed with a Combi-Flash® EZ Prep system (Teledyne ISCO, Lincoln, USA), using a MultoKrom® 100-5 C18 (CS-Chromatographie Service GmbH, Langerwehe, Germany) preparative column (20 × 150 mm, 5 µm) and the mobile phase consisting of 0.1% (v/v) formic acid (A) and 0.1% (v/v) formic acid in acetonitrile (B). For the separation, the following binary gradient elution program was applied (% B): 5 within 7 min; 5–95 within 18 min. The flow rate was set to 18 mL min$^{-1}$ and absorbance was detected at 200 nm. The fractions containing **5** were combined and evaporated, giving **5** as a formate salt.

Preparative kinetic resolution of *rac*-**5** for obtaining enantiopure remaining (*R*)-**5** was performed in a round-bottom flask with 8 mL reaction volume containing 0.2 M **4**, 0.5 mM PLP and 2.75 mg mL$^{-1}$ purified *Cv*-ATA L59A in 0.1 M $KP_i$ buffer (pH 7.5) at 30 °C with magnetic stirring. A solution of 0.5 M *rac*-**5** in 0.1 M $KP_i$ buffer (pH 7.5) was added dropwise over 15 min to give a final concentration of 0.2 M.

For obtaining enantiopure remaining (*S*)-**5** or (*S*)-**6**, the kinetic resolution was performed in a round-bottom flask with 10 mL or 3.3 mL reaction volume, respectively, containing 1.2 M **12**, 0.5 mM PLP and 30 mg mL$^{-1}$ ATA-117-Rd11 CFE in 0.1 M $KP_i$ buffer (pH 8.5) at 45 °C with magnetic stirring. 0.4 M *rac*-**5** or *rac*-**6**, respectively, in 0.1 M $KP_i$ buffer (pH 8.5) was added dropwise over 12 min or 15 min, respectively, to give a final concentration of 0.1 M.

The efficiency of the resolution was monitored by chiral HPLC analysis. The extraction was performed as described above, giving enantiopure (*R*)- and (*S*)-**5**, or (*S*)-**6**, respectively, as slightly brownish oils. See also figure captures for specific conditions regarding analytical scale reactions.

Direct synthesis of (*S*)-**6** was performed in a round-bottom flask with 9 mL reaction volume containing 1.5 M **11**, 50 mM **9**, 0.5 mM PLP, 20% DMSO and 4.8 mg mL$^{-1}$ purified *Cv*-ATA L59A in 0.1 M $KP_i$ buffer (pH 8.0) at 30 °C under magnetic stirring for 24 h. The pH was maintained at 8.0 with 4 M **11**. A 0.5 M solution of **9** in DMSO was added dropwise over 60 min to give a final concentration of 50 mM. Extraction was performed as described above with minor modifications: the residual DMSO was removed by re-extraction of the final organic fraction with water and brine. After the solvent evaporation, the extract was uploaded onto 2 preparative 0.5 mm TLC plates and run in the solvent system containing chloroform, methanol and 25% (v/v) ammonia (ratio 8:2:0.2). Elution of the sample from silica followed by the evaporation of volatiles yielded (*S*)-**6** as a yellow oil. See also figure captures for specific conditions regarding analytical scale reactions.

## Acknowledgements

*This project has received funding through The German Federal Ministry of Education and Research (BMBF), grant N°031B0595 and the initiative ERA CoBioTech (European Union's Horizon 2020 Research and Innovation Programme, grant N°722361). We gratefully acknowledge Eric Bräuchl, Nadya Abbood, Sarah Engel, Miriam Boeck and Daniel Klewinghaus for their contributions to preliminary experimental studies. We also thank Michael Kickstein for assistance in enzyme sample preparation.* Open access funding enabled and organized by Projekt DEAL.

## References

[1] a) O. I. Afanasyev, E. Kuchuk, D. L. Usanov, D. Chusov, *Chem. Rev.* **2019**, *119*, 11857–11911; b) S. Slagman, W. D. Fessner, *Chem. Soc. Rev.* **2021**, *50*, 1968–2009; c) A. Hager, N. Vrielink, D. Hager, J. Lefranc, D. Trauner, *Nat. Prod. Rep.* **2016**, *33*, 491–522.

[2] a) N. A. McGrath, M. Brichacek, J. T. Njardarson, *J. Chem. Educ.* **2010**, *87*, 1348–1349; b) J. Njardarson, **2020**, https://njardarson.lab.arizona.edu/content/top-pharmaceuticals-poster.

[3] a) H. Ohbayashi, *Expert Opin. Invest. Drugs* **2002**, *11*, 965–980; b) L. Storace, L. Anzalone, P. N. Confalone, W. P. Davis, J. M. Fortunak, M. Giangiordano, J. J. Haley, K. Kamholz, H. Y. Li, P. Ma, W. A. Nugent, R. L. Parsons, P. J. Sheeran, C. E. Silverman, R. E. Waltermire, C. C. Wood, *Org. Process Res. Dev.* **2002**, *6*, 54–63.

[4] a) K. M. Lee, P. Le, S. A. Sieber, S. M. Hacker, *Chem. Commun.* **2020**, *56*, 2929–2932; b) L. F. Peterson, H.

Sun, Y. Liu, H. Potu, M. Kandarpa, M. Ermann, S. M. Courtney, M. Young, H. D. Showalter, D. Sun, A. Jakubowiak, S. N. Malek, M. Talpaz, N. J. Donato, *Blood* **2015**, *125*, 3588–3597.

[5] a) H. Ishikawa, S. Shiomi, *Org. Biomol. Chem.* **2016**, *14*, 409–424; b) Z. L. Wang, *Molecules* **2019**, *24*, 3412.

[6] Q. Yin, Y. Shi, J. Wang, X. Zhang, *Chem. Soc. Rev.* **2020**, *49*, 6141–6153.

[7] a) S. A. Kelly, S. Mix, T. S. Moody, B. F. Gilmore, *Appl. Microbiol. Biotechnol.* **2020**, *104*, 4781–4794; b) M. D. Patil, G. Grogan, A. Bommarius, H. Yun, *Catalysts* **2018**, *8*, 254; c) F. Guo, P. Berglund, *Green Chem.* **2017**, *19*, 333–360.

[8] F. Steffen-Munsberg, C. Vickers, H. Kohls, H. Land, H. Mallin, A. Nobili, L. Skalden, T. van den Bergh, H.-J. Joosten, P. Berglund, M. Höhne, U. T. Bornscheuer, *Biotechnol. Adv.* **2015**, *33*, 566–604.

[9] J. S. Shin, B. G. Kim, *J. Org. Chem.* **2002**, *67*, 2848–2853.

[10] A. Telzerow, J. Paris, M. Hakansson, J. Gonzalez-Sabin, N. Rios-Lombardia, M. Schurmann, H. Groger, F. Moris, R. Kourist, H. Schwab, K. Steiner, *ACS Catal.* **2019**, *9*, 1140–1148.

[11] a) F. Steffen-Munsberg, C. Vickers, A. Thontowi, S. Schatzle, T. Meinhardt, M. S. Humble, H. Land, P. Berglund, U. T. Bornscheuer, M. Hohne, *ChemCatChem* **2013**, *5*, 154–157; b) E.-S. Park, M. Kim, J.-S. Shin, *Appl. Microbiol. Biotechnol.* **2012**, *93*, 2425–2435.

[12] E. S. Park, S. R. Park, S. W. Han, J. Y. Dong, J. S. Shin, *Adv. Synth. Catal.* **2014**, *356*, 212–220.

[13] a) C. K. Savile, J. M. Janey, E. C. Mundorff, J. C. Moore, S. Tam, W. R. Jarvis, J. C. Colbeck, A. Krebber, F. J. Fleitz, J. Brands, P. N. Devine, G. W. Huisman, G. J. Hughes, *Science* **2010**, *329*, 305–309; b) J. M. Janey, in *Sustainable Catalysis: Challenges and Practices for the Pharmaceutical and Fine Chemical Industries* (Eds.: P. J. Dunn, K. K. Hii, M. J. Krische, M. T. Williams), John Wiley & Sons, Inc., **2013**, pp. 75–88; c) L. J. Guan, J. Ohtsuka, M. Okai, T. Miyakawa, T. Mase, Y. Zhi, F. Hou, N. Ito, A. Iwasaki, Y. Yasohara, M. Tanokura, *Sci. Rep.* **2015**, *5*, 10753.

[14] a) S. W. Han, E. S. Park, J. Y. Dong, J. S. Shin, *Adv. Synth. Catal.* **2015**, *357*, 2712–2720; b) S. W. Han, E. S. Park, J. Y. Dong, J. S. Shin, *Adv. Synth. Catal.* **2015**, *357*, 1732–1740; c) A. Nobili, F. Steffen-Munsberg, H. Kohls, I. Trentin, C. Schulzke, M. Hohne, U. T. Bornscheuer, *ChemCatChem* **2015**, *7*, 757–760; d) I. V. Pavlidis, M. S. Weiss, M. Genz, P. Spurr, S. P. Hanlon, B. Wirz, H. Iding, U. T. Bornscheuer, *Nat. Chem.* **2016**, *8*, 1076–1082; e) J.-S. Shin, E.-S. Park, S. Han, (Univ Yonsei IACF), EP 3085776, **2016**; f) M. S. Weiss, I. V. Pavlidis, P. Spurr, S. P. Hanlon, B. Wirz, H. Iding, U. T. Bornscheuer, *ChemBioChem* **2017**, *18*, 1022–1026; g) A. W. H. Dawood, J. Bassut, R. O. M. A. de Souza, U. T. Bornscheuer, *Chem. Eur. J.* **2018**, *24*, 16009–16013; h) S. J. Novick, N. Dellas, R. Garcia, C. Ching, A. Bautista, D. Homan, O. Alvizo, D. Entwistle, F. Kleinbeck, T. Schlama, T. Ruch, *ACS Catal.* **2021**, *11*, 3762–3770.

[15] a) J. S. Shin, B. G. Kim, *Biosci. Biotechnol. Biochem.* **2001**, *65*, 1782–1788; b) P. Tufvesson, J. S. Jensen, W. Kroutil, J. M. Woodley, *Biotechnol. Bioeng.* **2012**, *109*, 2159–2162; c) H. Land, F. Ruggieri, A. Szekrenyi, W. D. Fessner, P. Berglund, *Adv. Synth. Catal.* **2020**, *362*, 812–821.

[16] J. S. Shin, B. G. Kim, *Biotechnol. Bioeng.* **1998**, *60*, 534–540.

[17] S. W. Han, J. Kim, H. S. Cho, J. S. Shin, *ACS Catal.* **2017**, *7*, 3752–3762.

[18] U. Kaulmann, K. Smithies, M. E. B. Smith, H. C. Hailes, J. M. Ward, *Enzyme Microb. Technol.* **2007**, *41*, 628–637.

[19] T. Scheidt, H. Land, M. Anderson, Y. Chen, P. Berglund, D. Yi, W.-D. Fessner, *Adv. Synth. Catal.* **2015**, *357*, 1721–1731.

[20] Y. V. Sheludko, W. D. Fessner, *Curr. Opin. Struct. Biol.* **2020**, *63*, 123–133.

[21] S. Schatzle, M. Hohne, E. Redestad, K. Robins, U. T. Bornscheuer, *Anal. Chem.* **2009**, *81*, 8244–8248.

[22] a) L. Leipold, D. Dobrijevic, J. W. E. Jeffries, M. Bawn, T. S. Moody, J. M. Ward, H. C. Hailes, *Green Chem.* **2019**, *21*, 75–86; b) D. Baud, N. Ladkau, T. S. Moody, J. M. Ward, H. C. Hailes, *Chem. Commun.* **2015**, *51*, 17225–17228.

[23] F. G. Mutti, C. S. Fuchs, D. Pressnitz, J. H. Sattler, W. Kroutil, *Adv. Synth. Catal.* **2011**, *353*, 3227–3233.

[24] a) P. Tufvesson, C. Bach, J. M. Woodley, *Biotechnol. Bioeng.* **2014**, *111*, 309–319; b) P. Tufvesson, J. Lima-Ramos, J. S. Jensen, N. Al-Haque, W. Neto, J. M. Woodley, *Biotechnol. Bioeng.* **2011**, *108*, 1479–1493.

[25] a) Y. Satyawali, D. F. del Pozo, P. Vandezande, I. Nopens, W. Dejonghe, *Biotechnol. Prog.* **2019**, *35*; b) P. Kelefiotis-Stratidakis, T. Tyrikos-Ergas, I. V. Pavlidis, *Org. Biomol. Chem.* **2019**, *17*, 1634–1642.

[26] J. S. Amato, R. J. Cvetovich, F. W. Hartner, (Merck & Co., Inc.), US 5808056, **1998**.

[27] U. Schell, R. Wohlgemuth, J. M. Ward, *J. Mol. Catal. B* **2009**, *59*, 279–285.

[28] A. O. Magnusson, A. Szekrenyi, H. J. Joosten, J. Finnigan, S. Charnock, W. D. Fessner, *FEBS J.* **2019**, *286*, 184–204.

[29] G. Shin, S. Mathew, H. Yun, *J. Ind. Eng. Chem.* **2015**, *23*, 128–133.

[30] H. G. Kim, S. W. Han, J. S. Shin, *Adv. Synth. Catal.* **2019**, *361*, 2594–2606.

[31] K. E. Cassimjee, C. Branneby, V. Abedi, A. Wells, P. Berglund, *Chem. Commun.* **2010**, *46*, 5569–5571.

[32] F. W. Studier, *Protein Expression Purif.* **2005**, *41*, 207–234.

[33] F. Subrizi, L. Benhamou, J. Ward, T. Sheppard, H. C. Hailes, *Angew. Chem. Int. Ed.* **2019**, *58*, 3854–3858; *Angew. Chem.* **2019**, *131*, 3894–3898.

[34] M. T. Davies, *Analyst* **1959**, *84*, 248–251.